

# Production of Photocatalytic Membranes by Supercritical Phase Inversion for the Removal of Antibiotics from Waste-Water

Mariangela Guastaferra<sup>a</sup>, Vincenzo Vaiano<sup>b,\*</sup>, Lucia Baldino<sup>b</sup>, Stefano Cardea<sup>b</sup>, Ernesto Reverchon<sup>b</sup>

<sup>a</sup>Department of Civil and Industrial Engineering, University of Pisa, Lungarno Pacinotti 43, 56126 Pisa, Italy.

<sup>b</sup>Department of Industrial Engineering, University of Salerno, Via Giovanni Paolo II, 84084, Fisciano (SA), Italy.

[vaiano@unisa.it](mailto:vaiano@unisa.it)

In recent years, scientific research has faced the numerous problems deriving from the presence of active ingredients in surface and groundwater. Traditional removal methods, such as adsorption and bioremediation, have several disadvantages; thus, in this work, membranes based on cellulose acetate loaded with Fe-N-TiO<sub>2</sub>, were tested for the photocatalytic degradation of Ceftriaxone Sodium from aqueous solution. The immobilization of the photocatalyst allows to overcome the limits of the photocatalytic process in suspension, which requires expensive and time-consuming post-treatments. Membranes were obtained by supercritical CO<sub>2</sub> phase inversion process and were subjected to characterizations such as EDX, TGA, FT-IR, Raman spectroscopy and, subsequently, tested in adsorption tests in the dark and in the presence of visible light, to evaluate their photocatalytic activity. The variations in the concentration of the antibiotic, during the tests conducted, were monitored by HPLC chromatographic analysis. Samples with 10% and 30% by weight of Fe-N-TiO<sub>2</sub> demonstrated relatively low adsorption efficiencies of the target contaminant, respectively equal to 22% and 18% in 180 minutes, for reasons related both to the morphology of the samples products, which changes from cellular to finger-like as the photocatalyst load increases, and to the quality of the dispersion. The membrane loaded with 20% by weight of Fe-N-TiO<sub>2</sub> allowed a degradation of the model pollutant of 35% in 180 minutes; moreover, the reusability of the membranes was verified. The photocatalytic tests showed that the photocatalytic efficiency was highly correlated to the dispersion of the photocatalyst nanoparticles and to its loading in the polymeric membranes.

## 1. Introduction

Pharmaceutical substances, a significant group of new environmental pollutants, have sparked heightened concerns due to their widespread presence in surface waters and wastewaters. Antibiotics and anti-inflammatory drugs are commonly found among these contaminants, and their removal rate through traditional treatments remains notably low (Raicopol et al., 2019). Polymer membrane technology is considered a promising method for the removal of pharmaceutical contaminants from wastewater (Wang et al., 2018). Indeed, this process provides membrane having high removal efficiency at a lower energy cost. Although cellulose acetate (CA) is a widely used polymer for crafting porous polymeric membranes, it has certain drawbacks, including low water permeability and poor mechanical properties. (El Gendy et al., 2017). Additives enhance pore quantity, area, the membrane's hydrophilic nature, and boost water permeability, thereby increasing water flow while preventing swelling (Simone et al., 2010). Nano-titanium dioxide (TiO<sub>2</sub>) has emerged as best candidate for producing nano-composite membranes in wastewater treatment due to its photocatalytic nature and hydrophilic properties. TiO<sub>2</sub> nanomaterial is frequently used in membrane production owing to its antifouling properties, hydrophilicity, and long-term stability. Additionally, TiO<sub>2</sub> nanoparticles have been identified as beneficial hydrophilic additives for reinforcing the mechanical attributes of polymeric membranes (Aljawrneh et al., 2022). Aljawrneh et al. (2022) processed cellulose acetate membranes treated

with titanium dioxide and cerium dioxide ( $\text{CeO}_2$ ) nanoparticles to enhance membrane photocatalytic activity. The nanocomposite membranes were synthesized using the phase inversion method and were tested for photocatalytic degradation of Methylene Blue (MB) by exposing the membrane/MB dye combination to UV illumination for different exposure times (up to 120 minutes). The SEM cross-sectional images revealed the presence of closed and not interconnected pores. The highest photocatalytic degradation activity was observed for CA– $\text{TiO}_2$  membrane with the photocatalytic activity of 64.0%. Meanwhile, the lowest activity was observed for CA– $\text{CeO}_2$  membrane (7.0%). Peixoto et al. (2020) synthesized cellulose acetate/silica/titania (CA/ $\text{SiO}_2/\text{TiO}_2$ ) and cellulose acetate/titania (CA/ $\text{TiO}_2$ ) based membranes, by the coupling of sol-gel technology and a modified version of the phase inversion technique. SEM micrographs confirmed the integral asymmetric structure of all membranes and permeation experiments revealed that the introduction of titania in the membranes did not improve the water permeation when compared to the pristine membrane. Mousa et al. (2023) prepared cellulose acetate membranes loaded with zinc oxide and  $\text{TiO}_2$  nanoparticles and they were tested for water disinfection from living organisms. Nanofibers were produced using the electrospinning method processing a solution flow rate of 1 mL/h and they showed a dye (MB) removal percentage of almost 20% during photocatalyst process.

Therefore, the aim of this work was to develop CA membranes loaded with Fe-N doped  $\text{TiO}_2$  nanoparticles by SC- $\text{CO}_2$  assisted phase inversion with the aim of providing an opened and interconnected polymeric structure, characterized by a good Fe-N- $\text{TiO}_2$  dispersion to remove a model antibiotic (i.e., ceftriaxone sodium) from an aqueous solution. Indeed, SC- $\text{CO}_2$ -assisted phase inversion process had already showed the capability of generating loaded membranes with high performances for several applications (Baldino et al., 2023; Cardea et al., 2019). Indeed, the interaction between the solvent in which polymer and nanocatalyst are suspended and non-solvent (SC- $\text{CO}_2$ ) triggers a phase transition, leading to polymer precipitation and the formation of porous interconnected structures. Replacing the liquid non-solvent with SC- $\text{CO}_2$  offers numerous advantages, in particular, SC- $\text{CO}_2$  can dry the structure without causing collapse of polymeric matrix, since it lacks the liquid-liquid interface. Moreover, its versatility enables easy modulation of structure morphology and cell size by adjusting operational conditions. This process eliminates the need for additional post-treatments and simplifies the recovery of the organic solvent. The experiments will be carried out to find the loading of Fe-N- $\text{TiO}_2$  nanoparticles that can guarantee the best catalyst dispersion in the polymeric support, the best adsorption-photocatalytic efficiency of the active membranes, and their reusability.

## 2. Materials and Methods

Cellulose acetate (CA, DA=2.44), acetone (purity > 99.5%), Ceftriaxone Sodium (CFX), Commercial  $\text{TiO}_2$  nanoparticles (PC 500),  $\text{CO}_2$  (99.9% purity) were supplied by Sigma-Aldrich (Milan, Italy), Millenium Inorganic Chemicals (Stallingborough, UK), and Morlando Group Srl (Sant'Antimo, Naples, Italy) respectively. Fe-N doped  $\text{TiO}_2$  were synthesized by sol-gel technique.  $\text{CO}_2$  (99.9% purity) was supplied by Morlando Group Srl (Sant'Antimo, Naples, Italy).

CA-based membranes were prepared by stabilizing 20 wt% of polymer in 10 mL of acetone. Fe-N- $\text{TiO}_2$  nanoparticles, at different percentage of Fe-N- $\text{TiO}_2$ /polymer by weight (10%, 20%, and 30%), were suspended in the polymeric solution and stirred at 100 rpm and 50 °C. The SC- $\text{CO}_2$  assisted phase inversion process was performed using a 316 stainless-steel cylindrical high-pressure vessel with an internal volume of 200 mL. This setup included a high-pressure pump (mod. LDB1, Lewa, Leonberg, Germany) responsible for delivering liquid  $\text{CO}_2$ . Pressure (set at 200 bar) within the vessel was monitored using a test gauge (mod. MP1, OMET, Lecco, Italy) and adjusted via a micrometering valve (mod. 1335G4Y, Hoke, Spartanburg, SC, USA). Process temperature was kept fixed at 35 °C. At the vessel's exit point, a rotameter was employed to measure the  $\text{CO}_2$  flow rate. The processes lasted 4 hours and the depressurization step required 30 minutes.

The membrane samples underwent cryo-fracturing using liquid nitrogen (SOL, Milan, Italy), followed by sputter coating with gold (Agar Auto Sputter Coater mod. 108 A, Stansted, UK) at 30 mA for 120 seconds. Subsequently, their morphology was examined using a field emission scanning electron microscope (FE-SEM, mod. LEO 1525, Carl Zeiss SMT AG, Oberkochen, Germany).

An energy-dispersive X-ray spectroscopy (EDX, mod. INCA Energy 350, Oxford Instruments) analysis was performed to identify Fe-N- $\text{TiO}_2$  clusters and their distribution in the polymeric support.

Tests for both adsorption and photocatalysis were conducted using an initial concentration of 50 mg/L of CFX in a 50 mL aqueous solution. The experiments were performed within a pyrex cylindrical photoreactor, measuring 2.6 cm in internal diameter and 9 cm in height. Adsorption and photocatalysis tests were conducted using CFX aqueous solution, initial concentration of 50 mg/L, in pyrex cylindrical reactor (2.6 cm X 9 cm). Light irradiation was provided by two lamps (Philips), with nominal power 8 W and emission range of wavelength 400-700 nm, put at 4 cm upper the surface of reactor (Figure 1). The overall reaction time lasted 180 minutes, conducted both in dark and light conditions. Analysis of the residual CFX concentration was carried out by

measuring its absorption at 270 nm using High-Pressure Liquid Chromatography (HPLC, Evolution 201, Thermo Scientific Fischer, Milan, Italy). A reusability test was performed after drying at room temperature of the 20wt% Fe-N-TiO<sub>2</sub>/CA membrane recovered from the treated aqueous solution at the end of the adsorption/photocatalytic process and reused without regeneration step among the different cycles.

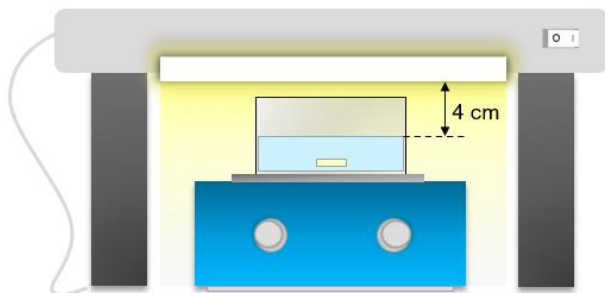


Figure 1. Set-up employed for adsorption and photocatalytic tests

### 3. Results and Discussion

In Figure 2, SEM images of 20wt% CA pure membranes (Figure 2a) and 30wt% Fe-N-TiO<sub>2</sub> loaded CA membranes (Figure 2b) are reported. Moreover, in Figure 2c an higher magnification of pore walls is shown.

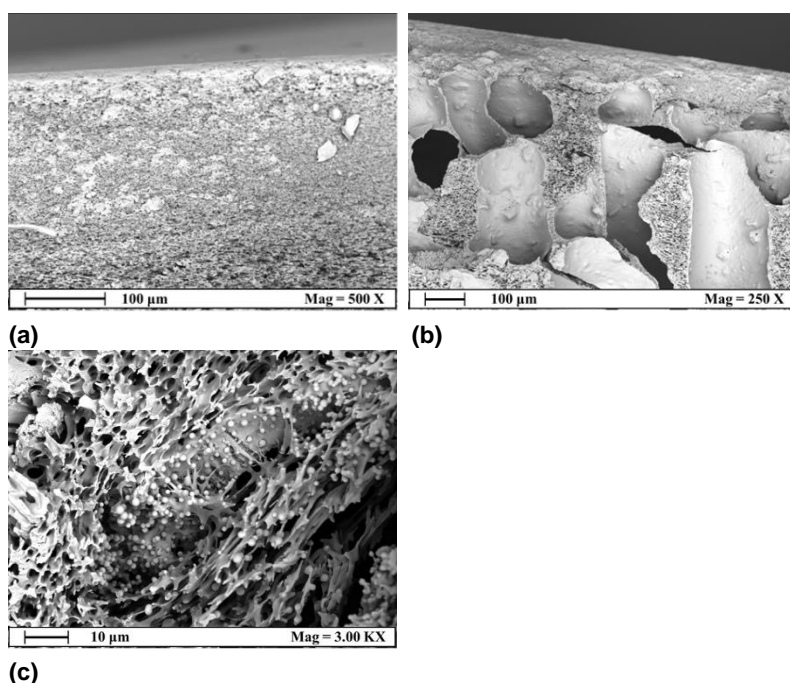


Figure 2. SEM images of pure 20wt% CA membranes (a), 30wt% Fe-N-TiO<sub>2</sub> loaded CA membranes (b) and zoom of inner pores present in b (c).

The SEM images revealed that, unlike the pure CA membrane (represented in figure 2a) characterized by a homogenous cellular structure, the loaded membranes exhibited macro-voids upon the increase of Fe-N-TiO<sub>2</sub> loading. This presence of macro-voids became noticeable as the percentage of photocatalyst relative to polymer increased up to 30wt%, forming a finger-like morphology (as shown in figure 2b). One possible explanation for this phenomenon is the thermodynamic instability occurring within the polymer-poor phase due to the introduction of TiO<sub>2</sub>-based nanoparticles. The photocatalytic nanoparticles acted as highly hydrophilic additives, promoting a fast L-L demixing in the starting solutions and consequently leading to the formation of macro-voids in the produced membranes (entering in the spinodal region of equilibrium diagram).

Furthermore, the inorganic particles interposed themselves among the polymer chains, enlarging the free volume fraction of the solution, that enhanced void formation (Guastaferrero et al., 2022). In Figure 3 EDX maps are reported to figure out how Fe-N-TiO<sub>2</sub> nanoparticles were distributed in the membranes section.

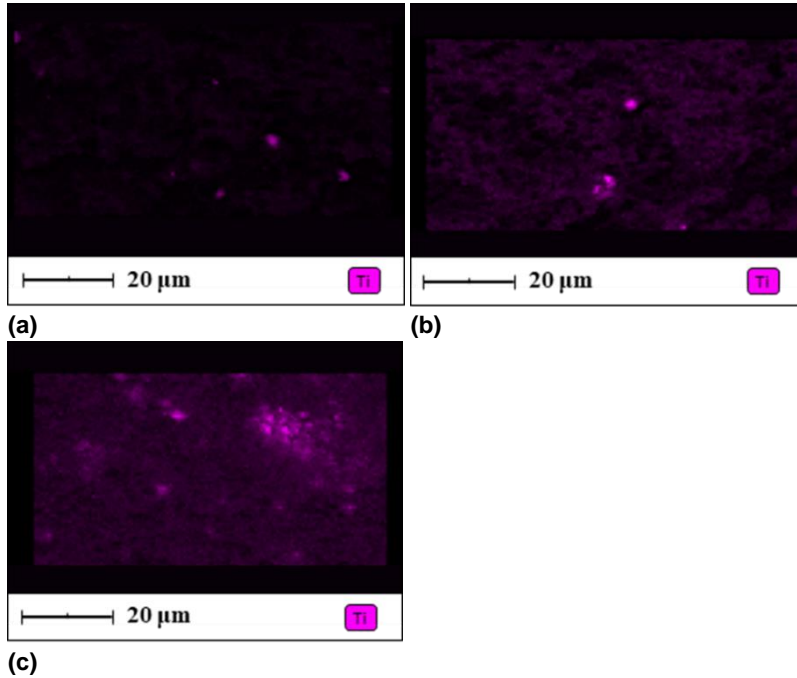


Figure 3. EDX analysis of 10wt% Fe-N-TiO<sub>2</sub> loaded CA membranes (a), 20wt% Fe-N-TiO<sub>2</sub> loaded CA membranes (b) and 30wt% Fe-N-TiO<sub>2</sub> loaded CA membranes (c).

These results showed that in Figure 3a (10wt% Fe-N-TiO<sub>2</sub>/CA membranes), it is possible to identify only a few amounts of Ti (detectable as violet spots), whereas a uniform dispersion of Fe, N and Ti elements in the entire section can be detected in Figure 3b (20wt% Fe-N-TiO<sub>2</sub>/CA membranes). Clusters of micrometric dimensions can be observed in Figure 3c (30wt% Fe-N-TiO<sub>2</sub>/CA membranes).

Figure 4 shows the curves related to CFX adsorption using Fe-N-TiO<sub>2</sub>/CA-based membranes; the adsorption tests were carried out either in the absence of light (Figure 4a) and after light exposure with a wavelength value ranging from 400 up to 700 nm as reported in Section 2 (Figure 4b).

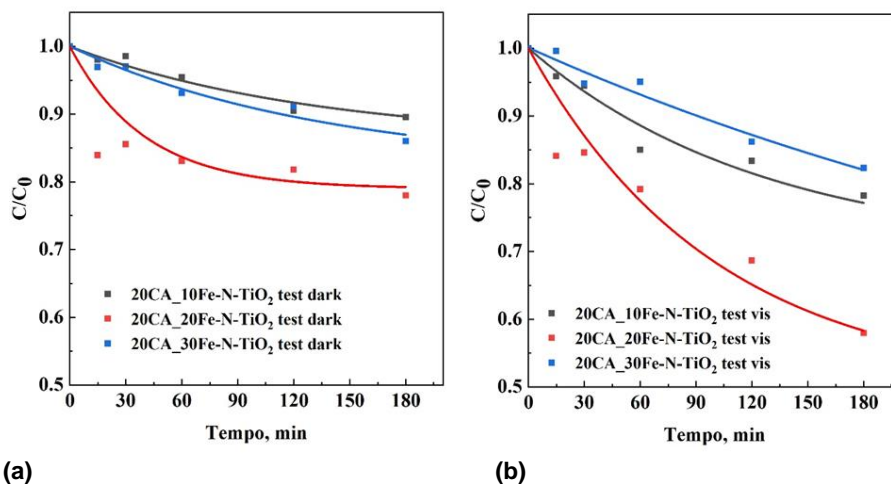


Figure 4. Adsorption curves of CFX related to 20wt% Fe-N-TiO<sub>2</sub> loaded CA membranes in dark conditions (a) and after Vis light exposure (b).

Figure 4a showed that the removal efficiency of CFX was low when adsorption tests were carried out in the absence of light. However, 20wt% Fe-N-TiO<sub>2</sub>/CA membrane exhibits higher adsorption rates compared to 10wt% and 30wt% Fe-N-TiO<sub>2</sub>/CA membranes. This result could be possibly attributed to a better and more uniform dispersion of the nanometer-scale photocatalyst (i.e., Fe-N-TiO<sub>2</sub>). This dispersion was also confirmed by EDX maps (Figure 3b). Indeed, improved dispersion tends to enhance the membrane's hydrophilic properties, thereby enhancing wettability and facilitating the diffusion of CFX within the porous structure until it reaches the active sites of Fe-N-TiO<sub>2</sub>. The membranes showed higher efficiency upon light exposure (Figure 4b), excluding 30wt% Fe-N-TiO<sub>2</sub>/CA membranes. This result could be explained considering clusters formation (Figure 3c), that reduced the number of available active sites due to a reduced catalyst specific surface area.

Figure 5 reports the last three cycles of reusability test using 20wt% Fe-N-TiO<sub>2</sub>/CA membrane to continue the CFX adsorption upon light exposure on the same membrane.

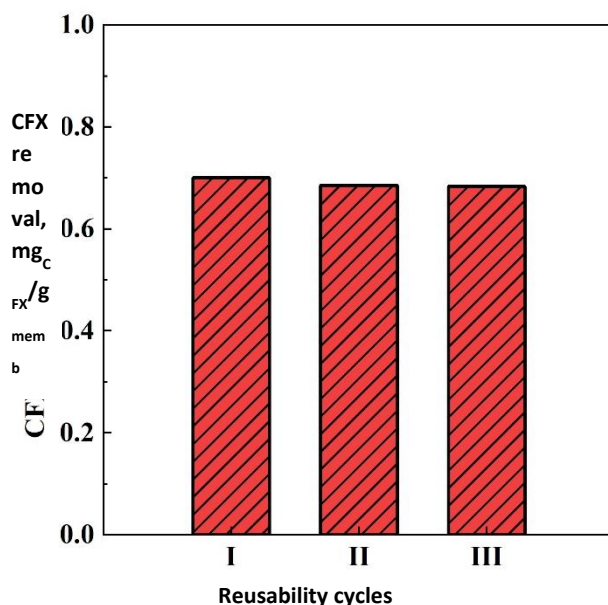


Figure 5. Reusability test (up to five adsorption cycles) of 20wt% Fe-N-TiO<sub>2</sub> loaded CA membranes.

After five consecutive cycles in the presence of visible light, the membrane continued to adsorb CFX. This result underlines that CA-loaded membranes continued its catalytic activity even after several photodegradative tests: adsorption kinetics related to the four regeneration cycles show mostly the same trend as the kinetics of the first photocatalytic test, demonstrating that the membrane is able to degrade the adsorbed CFX in an efficient manner even for repeated cycles; Moreover, due to the visible light irradiation, the membrane showed a good regeneration capacity at each cycle. This result showed that the photocatalytic oxidation process was able to degrade the adsorbed CFX molecules, preserving, at the same time, the original efficiency of the membrane.

#### 4. Conclusions

The membrane loaded with 20% by weight of Fe-N-TiO<sub>2</sub> allowed a degradation of the model pollutant of 35% in 180 minutes; moreover, the reusability of the membranes was verified. The photocatalytic tests showed that the photocatalytic efficiency was highly correlated to the dispersion of the photocatalyst nanoparticles and to its loading in the polymeric membranes. In next future, new experiments will be performed to find the key parameters to increase the degradation of the pollutant and other pollutants will be tested with this system.

#### References

Aljawrneh B., Alsaad A., Albiss B., Alrousan S., Alshanaheh A., Mutlaq S., 2022, Cellulose acetate membranes treated with titanium dioxide and cerium dioxide nanoparticles and their nanocomposites for enhanced photocatalytic degradation activity of methylene blue, *Journal of Materials Science: Materials in Electronics*, 33, 11420–11433.

- Baldino L., Gonzalez-Garcinuno A., Taberbero A., Cardea S., Martin Del Valle E., Reverchon E., 2023, Production of Cellulose Acetate Membranes Loaded with Quercetin by Supercritical CO<sub>2</sub> Phase Inversion, *Chemical Engineering Transactions*, 100, 475-480.
- Cardea S., Baldino L., Reverchon E., 2019, Production of PVDF-HFP Nanostructured Membranes for Water Purification by Supercritical Phase Inversion, *Chemical Engineering Transactions*, 73, 1-6.
- El-Gendi A., Abdallah H., Amin A., Amin S. K., 2017, Investigation of polyvinylchloride and cellulose acetate blend membranes for desalination, *Journal of Molecular Structure*, 1146, 14-22.
- Guastaferro M., Baldino L., Vaiano V., Cardea S., Reverchon E., 2022, Supercritical Phase Inversion to Produce Photocatalytic Active PVDF-coHFP\_TiO<sub>2</sub> Composites for the Degradation of Sudan Blue II Dye, *Materials*, 15(24), 8894-8909.
- Mousa S. A., Abdallah H., Khairy S. A., 2023, Low-cost photocatalytic membrane modified with green heterojunction TiO<sub>2</sub>/ZnO nanoparticles prepared from waste, *Scientific Reports*, 13, 22150.
- Peixoto I., Faria M., Gonçalves M. C., 2020, Synthesis and Characterization of Novel Integral Asymmetric Monophasic Cellulose–Acetate/Silica/Titania and Cellulose–Acetate/Titania Membranes, *Membranes*, 10(9), 195-221.
- Raicopol M.D., Andronescu C., Voicu S.I., Vasile E., Pandele A.M., 2019, Cellulose acetate/layered double hydroxide adsorptive membranes for efficient removal of pharmaceutical environmental contaminants, *Carbohydrate Polymers*, 214, 204-212.
- Simone S., Figoli A., Criscuoli A., Carnevale M.C., Rosselli A., Drioli E., 2010, Preparation of hollow fiber membranes from PVDF/PVP blends and their application in VMD, *Journal of Membrane Science*, 364, 219-232.
- Wang Y., Wang X., Li M., Dong J., Sun C., Chen G., 2018, Removal of Pharmaceutical and Personal Care Products (PPCPs) from Municipal Waste Water with Integrated Membrane Systems, MBR-RO/NF, *Int. J. Environ. Res. Public Health*, 15(2), 269-281.